JOURNAL OF THERMOPHYSICS AND HEAT TRANSFER
Vol. 13, No. 2, April–June 1999

Anisotropically Scattering Media Having a Reflective Upper Boundary

C. C. Liu* and R. L. Dougherty†
Oklahoma State University, Stillwater, Oklahoma 74078-5016

The objective of the present work is to obtain exact numerical solutions for radiative transfer in one-dimensional semi-infinite and finite anisotropically scattering media, with absorption but no emission, and having a Fresnel reflective upper boundary. The problem is simplified by solving for the desired functions only at the top boundary for the semi-infinite case, and at both boundaries for the finite case. The scattering phase function is represented by a series of Legendre polynomials. The principle of superposition as well as Ambarzumian's method are used in the solution process. A very abbreviated derivation is presented, and numerical results are obtained for semi-infinite and finite (up to 10) optical thicknesses for two albedoes (0.95 and 1), two refractive indices (1 and 1.33), and four selected phase functions. For these solutions, only information at the boundaries is obtained.

Nomenclature

B_k^m = function defined in Eq. (3)
D = function defined in Eq. (10)
I = intensity, W/m^2/sr
I_o = magnitude of the incident intensity just outside the upper boundary of the medium, W/m^2-sr
K_{ajmk} = Kernel functions defined in Eqs. (8) and (9), where a is either one or two
L = number of Legendre polynomials in phase-function representation
n = ratio of refractive index inside the medium (n_1) to that of the material (n_0) external to the upper boundary of the medium
P = scattering phase function defined in Eq. (2)
P_k^m = associated Legendre functions
P_{km} = source function defined in Eq. (6), W/m^2-sr
PP_{km} = source function defined in Eq. (11), W/m^2-sr
PP_{kma} = source functions defined in Eqs. (12) and (13), where a is either one or two, W/m^2-sr
q = flux, W/m^2
q_{km} = source function defined in Eq. (7), W/m^2-sr
R_{PPm} = reflection function defined in Eqs. (16) and (23), W/m^2-sr
S = source function defined in Eq. (5), W/m^2-sr
T_{PPIm} = transmission function defined in Eq. (24), W/m^2-sr
X_k = Legendre expansion coefficients
δ = Dirac delta function
δ_{0m} = Kronecker delta function
μ = direction cosine of the propagation angle of the radiation
ρ = interface reflection coefficient
τ = optical location
τ_0 = finite optical thickness
ϕ = azimuthal angle
ω = single-scattering albedo

Subscripts
A = collimated boundary condition
e = emission
in = inside the medium
o = outside the medium
ν = frequency dependent

Superscripts
$+$ = in the positive τ direction
$-$ = in the negative τ direction

Received May 26, 1998; presented as Paper 98-2841 at the AIAA/ASME 7th Joint Thermophysics and Heat Transfer Conference, Albuquerque, NM, June 15–18, 1998; revision received Oct. 28, 1998; accepted for publication Oct. 28, 1998.

*Graduate Research Associate, School of Mechanical and Aerospace Engineering, EN 218. Student Member AIAA.

†Professor, School of Mechanical and Aerospace Engineering, EN 218. Associate Fellow AIAA.

Introduction

EXTENSIVE studies for radiative transfer exist in the open literature. However, although some researchers have presented approximate or simplified approaches to the problem of anisotropic scattering with refractive index effects, exact numerical solutions are nonexistent. Many researchers have either ignored or simplified the effect of anisotropic scattering because of its mathematical complexity, whereas others have neglected or simplified the refractive index effects. Nevertheless, the rigorous combination of these two factors has not been studied previously to obtain the exact numerical results. Some interesting or similar studies will be mentioned in this paper.

Some typical studies in one-dimensional geometry have been conducted.[1–8] For a semi-infinite plane–parallel medium with isotropic scattering, Haggag et al.[1] solved the radiative transfer problem by using trial functions based on Case's eigenvalues. Some numerical results for reflected, i.e., backscattered, intensity were included without considering the effects of refractive index. Based on the discrete-ordinate algorithm, Liang and Lewis[2] studied a sky radiance distribution model with a reflective lower boundary performing as Lambertian. Several radiance distribution figures were given while the scattering phase function was defined as the average of Rayleigh and aerosol scattering phase functions. Settle[3] considered the case for a plane–parallel atmosphere bounded by a more general non-Lambertian reflecting lower surface. A family of closed-form solutions was presented for intensity with isotropic scattering; however, no numerical results were given. Wang et al.[4] utilized a spline approximation algorithm to solve radiative transfer problems in a one-dimensional finite slab with anisotropic scattering. Numerical results for intensity and flux were provided without accounting for the effect of refractive index. The Nyström method was employed by Wu and Liou[5] to solve the integral equations for a finite two-layer slab with Fresnel interfaces and isotropic scattering. Numerical

results for hemispherical reflectivity and transmissivity were also included.

Two different conditions for plane–parallel media were discussed by Ambirajan and Look.[6] They made use of a backward Monte Carlo method to numerically solve for the reflected intensity for a finite thick medium with isotropic scattering and for a semi-infinite medium with linearly anisotropic scattering. Index of refraction was not considered. The derivation of the correlation transfer equation for dynamic light scattering (very similar to that of radiative transfer) was presented by Reguigui et al.[7] By using preaveraging theory, the numerical results for correlation (which is comparable with radiative intensity), were obtained for both finite and semi-infinite media with a reflective boundary at incident. The effects of refractive index as well as anisotropic scattering on the correlation function were considered and discussed. Degheidy[8] solved a radiative transfer problem for plane–parallel media with linear anisotropic scattering and reflective interfaces by using the Pomraning–Eddington variational method. Hemispherical reflectivity and transmissivity were calculated numerically only for isotropic scattering with a transparent left boundary and a reflecting right boundary.

For two-dimensional cylindrical media, Crosbie and Dougherty,[9] Crosbie and Shieh,[10] and Crosbie and Lee[11] focused their attention on semi-infinite media, whereas Crosbie and Dougherty,[12,13] Crosbie and Lee,[14] and Reguigui and Dougherty[15] paid attention to finite geometry media. Crosbie and Dougherty[9] applied the method of separation of variables to reduce the two-dimensional isotropic scattering problem to a one-dimensional one. Exact numerical solutions were presented, but the effects of refractive index were ignored. Numerical results for backscattered intensity and flux were given by Crosbie and Shieh[10] for an isotropically scattering medium with a reflective top boundary. The incident radiation was either β varying or Gaussian in spatial distribution being collimated and normal to the top boundary.

A modified Ambarzumian's method was utilized by Crosbie and Lee[11] to numerically solve for the backscattered intensity and flux for anisotropically scattering media without a reflective boundary. Three- and five-term scattering phase functions were chosen by the authors to get numerical solutions. Crosbie and Dougherty[12] derived the equations for source function and flux for anisotropically scattering media without reflective boundaries. The phase function was represented in general as a finite sum of Legendre polynomials. No numerical results were given. Intensity and flux were numerically obtained by Crosbie and Dougherty[13] at the boundaries for linearly anisotropic scattering media. Refractive index effects were not included. Crosbie and Lee[14] gave the numerical results for intensity and flux for an anisotropically scattering medium without considering refractive index effects. The scattering phase function, chosen by the authors, depended on both the particle size and the refractive index of the particle. Reguigui and Dougherty[15] numerically solved for the intensity for a cylindrical layered medium with isotropic scattering and reflecting boundaries between the layers. The computer codes developed by authors could handle a medium having up to four layers.

For two-dimensional rectangular enclosures, Ramankutty and Crosbie,[16] Kim and Lee,[17,18] and Mitra et al.[19] focused their attention on the numerical solutions for heat flux. A wide variety of resources were provided by Ramankutty and Crosbie for two-dimensional rectangular media with and without scattering. Ramankutty and Crosbie used a modified discrete ordinates method to obtain the numerical results of heat flux for isotropically scattering media with the walls being all black. By using the discrete ordinates method, Kim and Lee[17] approximated the heat flux for an anisotropically scattering medium with diffusely reflecting walls. Numerical results were obtained by using four different anisotropically scattering phase functions. Kim and Lee[18] utilized the discrete ordinates method to numerically solve for the heat flux for an anisotropically scattering medium. The geometry was composed of a transparent top wall and three opaque walls.

A transient radiative transport problem was studied by Mitra et al.[19] for a scattering–absorbing medium. The P_1 approximation was applied to numerically solve for the heat flux.

For three-dimensional geometry, Crosbie and Shieh[20] and Kim and Baek[21] worked on the radiative transfer problem with anisotropically, and isotropically and anisotropically scattering media, respectively. Crosbie and Shieh[20] reduced the three-dimensional problem to a one-dimensional one by using a double Fourier transform. Refractive index effects were considered by the authors; however, no numerical results were given. By using the finite volume method, Kim and Baek numerically solved for the heat flux with the wall enclosures being black. The geometries for both axisymmetric and nonaxisymmetric cylindrical enclosures were discussed.

Special attention was paid to the effects of the refractive index by Spuckler and Siegel,[22,23] Siegel and Spuckler,[24] and Siegel[25–27] for either isotropic scattering or nonscattering media including emission. Spuckler and Siegel[22,23] and Siegel and Spuckler[24] examined problems with the geometry being a one-dimensional plane layer, two plane layers, and n plane layers; whereas Siegel[25–27] studied the geometry of a one-dimensional plane layer, a plane layer, and a two-dimensional rectangular solid. Numerical results were presented for temperature, temperature and flux, or emittance.

Presented herein is the solution for a one-dimensional plane–parallel medium exposed to collimated incident radiation on a (Fresnel) reflective upper boundary. The lower boundary is not reflective, and the material beyond that boundary is assumed to be nonparticipating. The medium absorbs and scatters anisotropically, but does not emit. The scattering phase function is represented by a series of Legendre polynomials. A very brief derivation of the equations to be solved is presented, and exact numerical flux and intensity results are presented for the problem formulated. These results show the effect of optical thickness, scattering albedo (absorption vs scattering), index of refraction, and anisotropic characteristics of the phase function. Selected results are also compared with solutions obtained by applying the modified P_n approximation to the problem.

Analysis

The radiative transport equation is[28]

$$\mu_{\text{in}}\, \mathrm{d}I_\nu(\tau, \mu_{\text{in}}, \phi_{\text{in}})/\mathrm{d}\tau + I_\nu(\tau, \mu_{\text{in}}, \phi_{\text{in}}) = (\omega_\nu/4\pi)\int_0^{2\pi}\int_{-1}^{1} I_\nu(\tau, \mu'_{\text{in}}, \phi'_{\text{in}})P(\mu'_{\text{in}}, \phi'_{\text{in}}, \mu_{\text{in}}, \phi_{\text{in}})\,\mathrm{d}\mu'_{\text{in}}\,\mathrm{d}\phi'_{\text{in}} = S_\nu(\tau, \mu_{\text{in}}, \phi_{\text{in}}) \tag{1}$$

for a one-dimensional medium, which scatters and absorbs without emitting (see Fig. 1). In Eq. (1), $P(\mu'_{\text{in}}, \phi'_{\text{in}}, \mu_{\text{in}}, \phi_{\text{in}})$ is the scattering phase function that can be expressed in general as a finite sum of Legendre polynomials[12]:

$$P(\mu'_{\text{in}}, \phi'_{\text{in}}, \mu_{\text{in}}, \phi_{\text{in}}) = \sum_{m=0}^{L}(2 - \delta_{0m})\sum_{k=m}^{L} B_k^m P_k^m(\mu_{\text{in}})P_k^m(\mu'_{\text{in}}) \times \cos[m(\phi_{\text{in}} - \phi'_{\text{in}})] \tag{2}$$

where

$$B_k^m = X_k[(k - m)!/(k + m)!] \tag{3}$$

In this paper, a collimated incident intensity exists at the upper boundary:

$$I_o^+(\mu'', \phi) = I_o\delta(\mu'' - \mu_o)\delta(\phi - \phi_o) \tag{4}$$

There is no radiation incident upon the lower boundary, and the material beyond the lower boundary has the same refractive index as that of the medium, but is assumed to be participating. Note that μ inside the medium is related to μ_o (outside the upper boundary of the medium) by Snell's law.[29]

By using an integrating factor to solve Eq. (1), as well as making use of the superposition method, the source function in Eq. (1) can be represented as[29]

$$S(\tau, \mu_{in}, \phi_{in}; \tau_0) = (\omega/4\pi) \sum_{m=0}^{L} (2 - \delta_{0m}) \sum_{k=m}^{L} B_k^m P_k^m(\mu_{in}) \times [\cos(m\phi_{in}) P_{km}(\tau; \tau_0) + \sin(m\phi_{in}) q_{km}(\tau; \tau_0)] \quad (5)$$

with the assumption that the incident azimuthal angle (ϕ_o) is equal to zero. Then

$$P_{km}(\tau, \mu, n; \tau_0) = D(\mu, n) P_k^m(\mu) e^{-\tau/\mu} + (\omega/2) \sum_{j=m}^{L} B_j^m \int_0^{\tau_0} P_{jm}(t, \mu, n; \tau_0)[(-1)^m K_{1jmk}(\tau + t, n) + K_{2jmk}(\tau - t)]\, dt \quad (6)$$

$$q_{km}(\tau, \mu, n; \tau_0) = (\omega/2) \sum_{j=m}^{L} B_j^m \int_0^1 \int_0^{\tau_0} \{(-1)^m \times q_{jm}(t, \mu, n; \tau_0) \exp[-(\tau + t)/\mu_{in}'] \rho(\mu_{in}', n) P_j^m(-\mu_{in}') \times P_k^m(\mu_{in}') + q_{jm}(t, \mu, n; \tau_0) \exp[-|\tau - t|/\mu_{in}'] \times P_j^m[\text{sign}(\tau - t)\mu_{in}'] P_k^m[\text{sign}(\tau - t)\mu_{in}']\}\, dt\, d\mu_{in}'/\mu_{in}' \quad (7)$$

where

$$K_{1jmk}(\tau + t, n) = \int_0^1 \exp[-(\tau + t)/\mu_{in}'] P_j^m(-\mu_{in}') \rho(\mu_{in}', n) \times P_k^m(\mu_{in}')\, d\mu_{in}'/\mu_{in}' \quad (8)$$

$$K_{2jmk}(\tau - t) = \int_0^1 \exp[-|\tau - t|/\mu_{in}'] P_j^m[\text{sign}(\tau - t)\mu_{in}'] \times P_k^m[\text{sign}(\tau - t)\mu_{in}']\, d\mu_{in}'/\mu_{in}' \quad (9)$$

$$D(\mu, n) = (\mu_o/\mu)[1 - \rho(\mu_o, 1/n)] I_o \quad (10)$$

and ρ is a generic interface reflection coefficient that will be represented herein by Fresnel's relationship.[29]

Equation (7) implies that the q_{km} function is equal to zero because there is no lead term, caused by ϕ_o being assigned the value zero. Therefore, only the P_{km} function needs to be solved to obtain the solutions of the proposed problem.

Semi-Infinite Medium

For infinite optical thickness, the fundamental source function is[29]

$$P_{km}(\tau, \mu, n) = D(\mu, n) PP_{km}(\tau, \mu, n) = D(\mu, n)[PP_{km1}(\tau, \mu) + PP_{km2}(\tau, \mu, n)] \quad (11)$$

where

$$PP_{km1}(\tau, \mu) = P_k^m(\mu) e^{-\tau/\mu} + (\omega/2) \sum_{j=m}^{L} B_j^m \int_0^{\infty} PP_{jm1}(t, \mu) K_{2jmk}(\tau - t)\, dt \quad (12)$$

$$PP_{km2}(\tau, \mu, n) = (\omega/2) \sum_{j=m}^{L} B_j^m (-1)^m \int_0^{\infty} PP_{jm}(t, \mu, n) K_{1jmk}(\tau + t, n)\, dt + (\omega/2) \sum_{j=m}^{L} B_j^m \int_0^{\infty} PP_{jm2}(t, \mu, n) K_{2jmk}(\tau - t)\, dt \quad (13)$$

After some manipulation, by mainly using the principle of superposition as well as Ambarzumian's method[30] in the solution process, the exact expressions for reflected (or backscattered) intensity and upper boundary flux become[29]

$$I_{Ae}^-(0, \mu_e, \mu_o, \phi_{in}, n) = [(I_o\mu_o)/2\pi][1 - \rho(\mu_o, 1/n)] \times \langle 1 - \rho\{[1 - (1 - \mu_e^2)/n^2]^{1/2}, n\}\rangle \times \sum_{m=0}^{L} (2 - \delta_{0m}) \cos(m\phi_{in}) R_{PPm}\{[1 - (1 - \mu_e^2)/n^2]^{1/2}, \mu, n\} / \{n^2\mu[1 - (1 - \mu_e^2)/n^2]^{1/2}\} \quad (14)$$

$$q(0, \mu_o, n) = P_{10}(0, \mu, n) \quad (15)$$

where $\mu = [1 - (1 - \mu_o^2)/n^2]^{1/2}$, and R_{PPm} is the reflection function that can be expressed as

$$R_{PPm}(\bar{\mu}, \mu, n) = [1/(1/\bar{\mu} + 1/\mu)](\omega/2) \sum_{k=m}^{L} B_k^m PP_{km1}(0, \mu) \times (-1)^{k+m} PP_{km1}(0, \bar{\mu}) + (\omega/2) \sum_{k=m}^{L} B_k^m (-1)^k \times PP_{km1}(0, \bar{\mu}) \int_0^1 [1/(1/\bar{\mu} + 1/\mu_{in}')] PP_{km1}(0, \mu_{in}') \times R_{PPm}(\mu_{in}', \mu, n) \rho(\mu_{in}', n)\, d\mu_{in}'/\mu_{in}' \quad (16)$$

With the help of the following two equations[29]:

$$PP_{jm1}(0, \mu) = P_j^m(\mu) + (\omega/2) \sum_{i=m}^{L} (-1)^{i+m} B_i^m PP_{im1}(0, \mu) \times \int_0^1 [1/(1/\mu_{in}' + 1/\mu)] PP_{im1}(0, \mu_{in}') P_j^m(-\mu_{in}')\, d\mu_{in}'/\mu_{in}' \quad (17)$$

$$PP_{km}(0, \mu, n) = P_k^m(\mu) + (\omega/2) \sum_{j=m}^{L} (-1)^j B_j^m PP_{jm1}(0, \mu) \times \int_0^1 [1/(1/\mu_{in}' + 1/\mu)] PP_{jm1}(0, \mu_{in}')[(-1)^m P_k^m(-\mu_{in}') + \rho(\mu_{in}', n) PP_{km}(0, \mu_{in}', n)]\, d\mu_{in}'/\mu_{in}' \quad (18)$$

the reflected intensity, flux, and reflection function can be determined numerically.

Finite Medium

Following a similar approach to that for the semi-infinite medium, the exact expressions for reflected (or backscattered) and transmitted (or forward-scattered) intensities and for fluxes can be deduced as[29]

$$I_{Ae}^-(0, \mu_e, \mu_o, \phi_{in}, n; \tau_0) = [(I_o\mu_o)/2\pi][1 - \rho(\mu_o, 1/n)] \times \langle 1 - \rho\{[1 - (1 - \mu_e^2)/n^2]^{1/2}, n\}\rangle \sum_{m=0}^{L} (2 - \delta_{0m}) \times \cos(m\phi_{in}) R_{PPm}\{[1 - (1 - \mu_e^2)/n^2]^{1/2}, \mu, n; \tau_0\} / \{n^2\mu[1 - (1 - \mu_e^2)/n^2]^{1/2}\} \quad (19)$$

$$I^{+}_{Ae}(\tau_0, \mu_{in}, \mu_o, \phi_{in}, n; \tau_0) = [(I_o\mu_o)/\mu][1 - \rho(\mu_o, 1/n)] \times \delta(\mu_{in} - \mu)\delta(\phi_{in} - \phi_o)e^{-\tau_0/\mu_{in}} + [(I_o\mu_o)/(2\pi\mu_{in}\mu)] \times [1 - \rho(\mu_o, 1/n)] \sum_{m=0}^{L} (2 - \delta_{0m})\{\rho(\mu_{in}, n)e^{-\tau_0/\mu_{in}} \times \cos[m(\phi_{in} + 180°)]R_{PPm}(\mu_{in}, \mu, n; \tau_0) + \cos(m\phi_{in})T_{PPlm}(\mu_{in}, \mu, n; \tau_0)\} \quad (20)$$

$$q(0, \mu_o, n; \tau_0) = P_{10}(0, \mu, n; \tau_0) \quad (21)$$

$$q(\tau_0, \mu_o, n; \tau_0) = P_{10}(\tau_0, \mu, n; \tau_0) \quad (22)$$

where $\mu = [1 - (1 - \mu_o^2)/n^2]^{1/2}$ (by Snell's Law), and R_{PPm} and T_{PPlm} are reflection and transmission functions that can be expressed as

$$R_{PPm}(\bar{\mu}, \mu, n; \tau_0) = [1/(1/\bar{\mu} + 1/\mu)](\omega/2) \times \sum_{k=m}^{L} (-1)^{k+m}B_k^m[PP_{km1}(0, \mu; \tau_0)PP_{km1}(0, \bar{\mu}; \tau_0) - PP_{km1}(\tau_0, \mu; \tau_0)PP_{km1}(\tau_0, \bar{\mu}; \tau_0)] + (\omega/2) \times \sum_{k=m}^{L} (-1)^kB_k^m \int_0^1 [1/(1/\bar{\mu} + 1/\mu'_{in})]R_{PPm}(\mu'_{in}, \mu, n; \tau_0) \times [PP_{km1}(0, \mu'_{in}; \tau_0)PP_{km1}(0, \bar{\mu}; \tau_0) - PP_{km1}(\tau_0, \mu'_{in}; \tau_0)PP_{km1}(\tau_0, \bar{\mu}; \tau_0)]\rho(\mu'_{in}, n)\, d\mu'_{in}/\mu'_{in} \quad (23)$$

$$T_{PPlm}(\bar{\mu}, \mu, n; \tau_0) = [1/(1/\bar{\mu} - 1/\mu)](\omega/2) \times \sum_{k=m}^{L} B_k^m[PP_{km1}(\tau_0, \mu; \tau_0)PP_{km1}(0, \bar{\mu}; \tau_0) - PP_{km1}(0, \mu; \tau_0)PP_{km1}(\tau_0, \bar{\mu}; \tau_0)] + (\omega/2) \times \sum_{k=m}^{L} (-1)^kB_k^m \int_0^1 [1/(1/\mu'_{in} + 1/\mu)]T_{PPlm}(\bar{\mu}, \mu'_{in}, n; \tau_0) \times [PP_{km1}(0, \mu; \tau_0)PP_{km1}(0, \mu'_{in}; \tau_0) - PP_{km1}(\tau_0, \mu; \tau_0)PP_{km1}(\tau_0, \mu'_{in}; \tau_0)]\rho(\mu'_{in}, n)\, d\mu'_{in}/\mu'_{in} \quad (24)$$

With the help of the following four equations[29]:

$$\partial PP_{km1}(0, \mu; \tau_0)/\partial\tau_0 = (\omega/2) \sum_{j=m}^{L} (-1)^{j+k}B_j^m \times PP_{jm1}(\tau_0, \mu; \tau_0) \int_0^1 PP_{km1}(\tau_0, \mu'_{in}; \tau_0)P_j^m(\mu'_{in})\, d\mu'_{in}/\mu'_{in} \quad (25)$$

$$\partial PP_{km1}(\tau_0, \mu; \tau_0)/\partial\tau_0 = -(1/\mu)PP_{km1}(\tau_0, \mu; \tau_0) + (\omega/2) \sum_{j=m}^{L} B_j^m PP_{jm1}(0, \mu; \tau_0) \int_0^1 PP_{km1}(\tau_0, \mu'_{in}; \tau_0) \times P_j^m(\mu'_{in})\, d\mu'_{in}/\mu'_{in} \quad (26)$$

$$PP_{km}(0, \mu, n; \tau_0) = PP_{km1}(0, \mu; \tau_0) + (\omega/2) \times \sum_{j=m}^{L} (-1)^jB_j^m \int_0^1 [1/(1/\mu'_{in} + 1/\mu)]PP_{km}(0, \mu'_{in}, n; \tau_0) \times [PP_{jm1}(0, \mu; \tau_0)PP_{jm1}(0, \mu'_{in}; \tau_0) - PP_{jm1}(\tau_0, \mu; \tau_0)PP_{jm1}(\tau_0, \mu'_{in}; \tau_0)]\rho(\mu'_{in}, n)\, d\mu'_{in}/\mu'_{in} \quad (27)$$

$$PP_{km}(\tau_0, \mu, n; \tau_0) = PP_{km1}(\tau_0, \mu; \tau_0) + (\omega/2) \times \sum_{j=m}^{L} (-1)^jB_j^m \int_0^1 [1/(1/\mu'_{in} + 1/\mu)]PP_{km}(\tau_0, \mu'_{in}, n; \tau_0) \times [PP_{jm1}(0, \mu; \tau_0)PP_{jm1}(0, \mu'_{in}; \tau_0) - PP_{jm1}(\tau_0, \mu; \tau_0)PP_{jm1}(\tau_0, \mu'_{in}; \tau_0)]\rho(\mu'_{in}, n)\, d\mu'_{in}/\mu'_{in} \quad (28)$$

the reflection and transmission functions, reflected and transmitted intensities, and fluxes can be numerically determined. Note that, as the optical thickness of the medium becomes infinite, Eq. (23) reduces to Eq. (16), and Eq. (27) reduces to Eq. (18).

Numerical Results

Some selected figures are presented giving numerical solutions of Eqs. (14) and (19–22), with the generic reflection coefficient (ρ) in those equations being that of Fresnel's. For these figures, the reflected and transmitted intensities are calculated only at the boundaries (Fig. 1). The reflected intensity represents only the intensity reflected from the medium caused by scattering within the medium, excluding the direct interface reflection of the incident radiation, i.e., $\rho(\mu, 1/n)I_o\delta(\mu - \mu_o)\delta(\phi_{in} - \phi_o)$; whereas the transmitted intensity excludes any part of the incident intensity that directly reaches the lower interface undisturbed, i.e., $(I_o\mu_o/\mu)[1 - \rho(\mu_o, 1/n)]\delta(\mu_{in} - \mu)\delta(\phi_{in} - \phi_o)e^{-\tau_0/\mu_{in}}$ of Eq. (20). In addition, the upper boundary flux actually represents the net flux at the upper boundary, excluding directly reflected incident radiation at that interface; whereas the transmitted flux excludes any part of the incident radiation reaching the lower interface undisturbed. Note that all intensities and fluxes presented are nondimensional, divided by I_o for intensity, and divided by πI_o for flux.

Moreover, for these examples, modifications of the phase functions suggested by Kim and Lee[17,18] are used and tabulated in Table 1. The phase function $B1$ (termed $B2$ by Kim and Lee[17]) in Table 1, is a backward-scattering phase function for small particles with very large refractive indices, whereas $F1$ (termed $F3$ by Kim and Lee[18]) is the forward-scattering counterpart of $B1$. Phase function $B2$ (termed $B1$ by Kim and Lee[17]) is the backward-scattering phase function for a particle size parameter of 1 with an infinite refractive index; whereas, according to Kim and Lee,[17] $F2$ is the forward-scattering phase function for a particle size parameter of 2 and a refractive index of 1.33. However, the last three coefficients of this phase function have been omitted herein, so that $L = 5$, the same as that of $B2$. If the $F2$ phase functions for $L = 8$ from Kim and Lee[17] and for $L = 5$ herein are compared, the maximum differences between the two phase functions are only 0.2% in the forward directions and 7% in the backward direction. Because $F2$ is forward scattering, scattering in the backward direction is one-tenth of the magnitude of that in the forward direction.

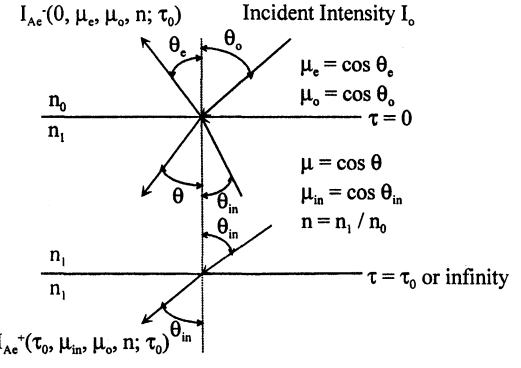

Fig. 1 Geometry of a one-dimensional medium with reflective upper boundary.

Therefore, our reduction of $F2$ from $L = 8$ to $L = 5$ should have minimal effect on flux and intensity for this case.

For the finite medium, a fifth-order Runge–Kutta algorithm was employed to solve Eqs. (25) and (26) with an optical thickness step size ($\Delta\tau_o$) of 0.0005, and a Gauss–Legendre quadrature of 100 points for integration. This large number of integration quadrature was needed because of the dramatic change in the Fresnel reflection coefficient (ρ) at the critical angle. The precise quadrature number was determined to be sufficient by running a case ($L = 2$, $\omega = 0.95$, $n = 1.33$, and $\tau_0 = 10$) with 128 quadrature, and finding that the worst error between the 100-point quadrature and the 128-point quadrature was a 10^{-7} fractional error.

After the solutions of Eqs. (25) and (26) were obtained, Eqs. (27) and (28) were solved iteratively; then Eqs. (23) and (24) were solved iteratively. Iterative convergence was based on the calculation of maximum iterative fractional error to be less than or equal to 10^{-8}. Finally, the reflection and transmission functions of Eqs. (23) and (24) were substituted into Eqs. (19) and (20) for intensity, and Eqs. (21) and (22) were used for flux. For the semi-infinite medium, Eqs. (17) and (18) were solved iteratively with a 100-point Gauss–Legendre quadrature. Then Eq. (16) was solved iteratively and substituted into Eq. (14) for reflected intensity, and Eq. (15) was used for flux.

Figures 2–4 show the effects of the number of Legendre polynomials (L), single-scattering albedo (ω), and refractive index (n) on the reflected, i.e., backscattered, and transmitted, i.e., forward-scattered, intensities by using the $B1$ and $F1$ phase functions.

As expected, the reflected intensity for $L = 2$ and $B1$ (backward scattering) is larger than the one for $L = 0$ (isotropic); whereas the transmitted intensity for $L = 2$ and $B1$ is smaller than that for $L = 0$ in Fig. 2. This is because the backward-scattering phase function tends to scatter toward the upper boundary and scatter away from the lower boundary. However, an opposite result is found in Fig. 2 for $F1$, because of forward-scattering phase-function effects.

Table 1 Expansion coefficients (X_k) of four anisotropic phase functions

k	$F1$	$F2$	$B1$	$B2$
0	1.000	1.00000	1.000	1.00000
1	1.200	2.00917	−1.200	−0.56524
2	0.500	1.56339	0.500	0.29783
3	——	0.67407	——	0.08571
4	——	0.22215	——	0.01003
5	——	0.04725	——	0.00063

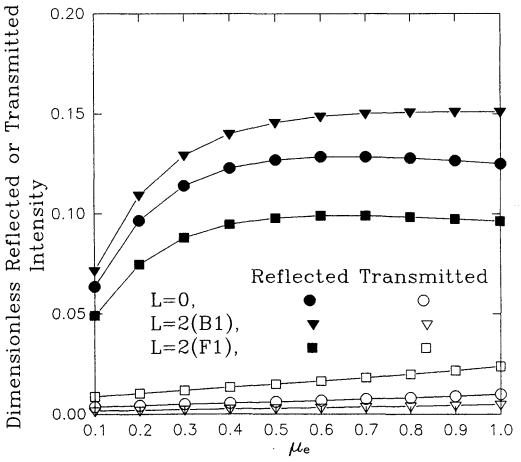

Fig. 2 Effect of number of Legendre polynomials on the nondimensional reflected and transmitted intensities for $F1$ and $B1$ phase functions ($n = 1.33$, $\omega = 0.95$, $\tau_0 = 10$).

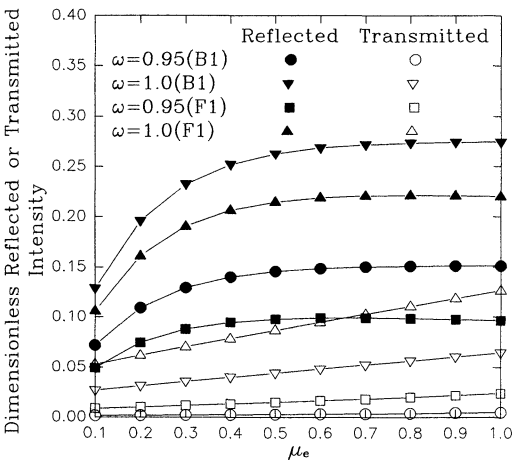

Fig. 3 Effect of single-scattering albedo on the nondimensional reflected and transmitted intensities for $F1$ and $B1$ phase functions ($n = 1.33$, $L = 2$, $\tau_0 = 10$).

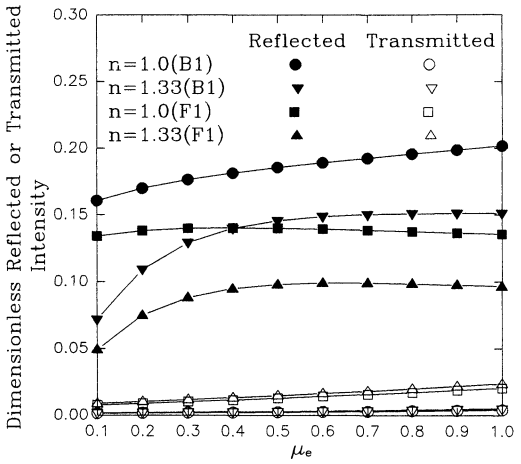

Fig. 4 Effect of refractive index on the nondimensional reflected and transmitted intensities for $F1$ and $B1$ phase functions ($L = 2$, $\omega = 0.95$, $\tau_0 = 10$).

Figure 3 reveals that the reflected and transmitted intensities increase as the single-scattering albedo increases. The reason is that a larger percentage of radiation will be scattered (and less will be absorbed) in the medium when the single-scattering albedo becomes greater. This effect will contribute to the intensities at both boundaries. For albedoes smaller than 0.95, the intensities and fluxes decrease very rapidly with decreasing albedo, because decreasing albedo indicates that the fraction of scattering decreases while the fraction of absorption increases (for constant optical thickness). In these lower albedo cases, the effects of optical thickness, refractive index, and phase function are similar in trend, but are considerably less dramatic, compared with the effects for the case of unit albedo.

Reflected intensity decreases and transmitted intensity increases as refractive index increases, as shown in Fig. 4. The major reason is that total internal reflection occurs for all μ values less than the critical μ value (or for angles greater than the critical angle, θ_{critical}), where $\mu_{\text{critical}} = (1 - n^{-2})^{0.5}$. Thus, the energy exiting the upper boundary decreases and that leaving the lower boundary increases, as μ_{critical} increases (or as θ_{critical} decreases), i.e., as refractive index increases.

Figures 5 and 6 demonstrate the effects of optical thickness (τ_0) on the reflected and transmitted intensities, respectively, using the $B1$ phase function; whereas Figs. 7 and 8 illustrate the same effects on intensities using the $F1$ phase function. The reflected intensity increases as optical thickness increases, as revealed by both Figs. 5 and 7. This is because of the reduced chances of scattering outside through the lower bound-

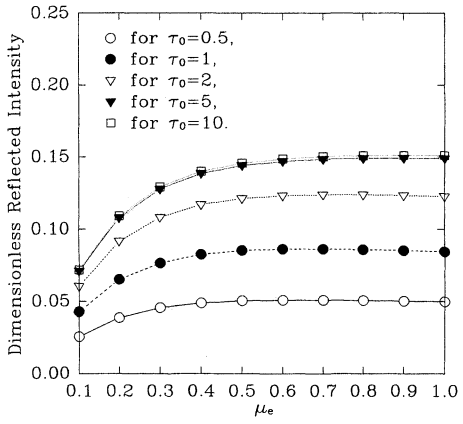

Fig. 5 Effect of optical thickness on the nondimensional reflected intensity for $B1$ phase function (n = 1.33, L = 2, ω = 0.95).

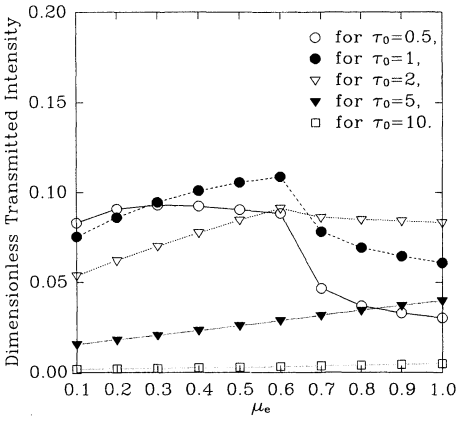

Fig. 6 Effect of optical thickness on the nondimensional transmitted intensity for $B1$ phase function (n = 1.33, L = 2, ω = 0.95).

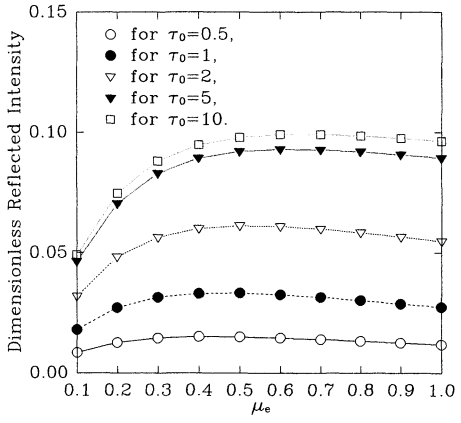

Fig. 7 Effect of optical thickness on the nondimensional reflected intensity for $F1$ phase function (n = 1.33, L = 2, ω = 0.95).

ary when optical thickness becomes larger, with improved chances of scattering outside through the upper boundary.

Figures 6 and 8 point out an interesting result. For all μ_e values, beginning at low optical thickness, the transmitted intensity first increases as optical thickness increases, peaks, and then decreases with further increases in optical thickness. The optical thickness at which the peak occurs is relatively small for smaller μ_e, and larger for larger μ_e. The explanation for this is that the intensity has a greater chance of scattering as optical thickness increases (which also varies as a function of μ_e, because of the effective optical path length being related to τ/μ_e), and we are plotting only scattered intensity (having removed the undisturbed portion). However, after a certain optical thickness, the transmitted intensity decreases. This is because the increased number of scattering events causes more radiation to scatter out from the upper boundary than from the lower boundary. Note that the critical angle effects (between μ_e = 0.6 and 0.7), which cause a rapid change for $\tau_0 \leq 2$ in both Figs. 6 and 8, are damped out for optical thickness greater than or equal to 5. Moreover, a more rapid change for $\tau_0 \leq 2$ in Fig. 6 is a result of the backward-scattering phase function emphasizing the effect of the upper boundary's refractive index.

Figures 9 and 10 show the effect of the number of Legendre polynomials (L) on the reflected and transmitted intensities when using the $B2$ and $F2$ phase functions, respectively. As expected, Figs. 9 and 10 have similar trends to those of Fig. 2. Moreover, for comparison with the L = 5 results, a P_n solution has been added to Fig. 9. Figure 9 shows modified P_5 predictions,[31] which corroborate the exact results presented herein. As expected from the modified P_n solution technique, its results for intensity are qualitatively quite good, but are quantitatively in error.

Figures 11 and 12 show the effect of optical thickness (τ_0) on the upper boundary and transmitted fluxes, respectively, using the $F1$ phase function. As might be expected, Figs. 11 and 12 have similar general trends to those of Figs. 7 and 8, in that, for small enough τ_0, the radiation (intensity or flux) increases with increasing τ_0, peaks, then decreases for larger values of τ_0. (The peak τ_0 value depends on the μ value of interest.) Figure 11 shows that, as optical thickness increases, the flux at the upper boundary reaches a maximum level. Thus, it can be deduced that the upper boundary flux for an infinitely

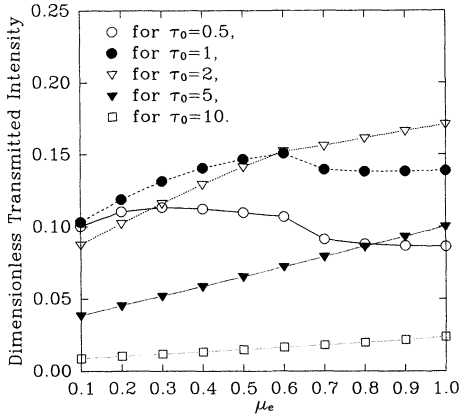

Fig. 8 Effect of optical thickness on the nondimensional transmitted intensity for $F1$ phase function (n = 1.33, L = 2, ω = 0.95).

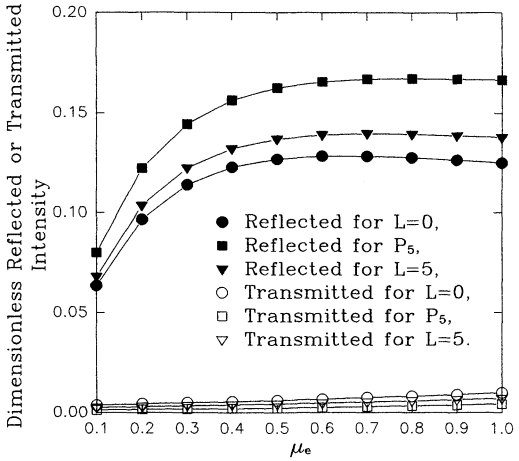

Fig. 9 Effect of number of Legendre polynomials as compared with the P_n approximation on the nondimensional reflected and transmitted intensities for $B2$ phase function (n = 1.33, ω = 0.95, τ_0 = 10).

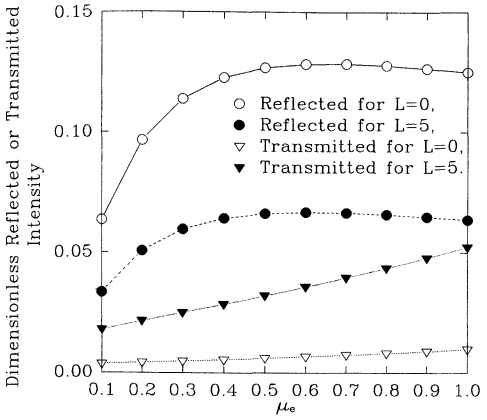

Fig. 10 Effect of number of Legendre polynomials on the nondimensional reflected and transmitted intensities for $F2$ phase function (n = 1.33, ω = 0.95, τ_0 = 10).

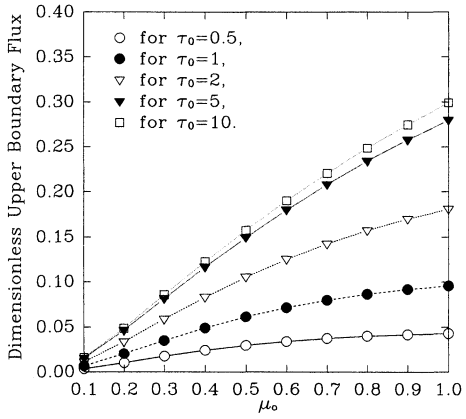

Fig. 11 Effect of optical thickness on the nondimensional upper boundary flux for $F1$ phase function (n = 1.33, L = 2, ω = 0.95).

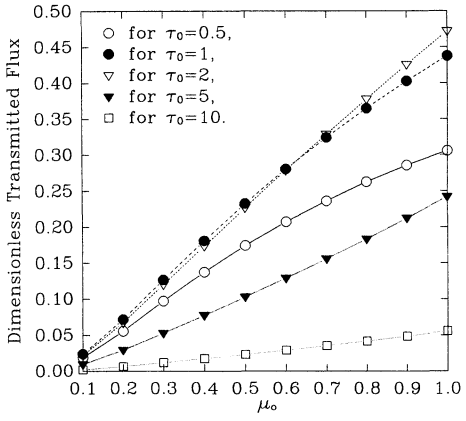

Fig. 12 Effect of optical thickness on the nondimensional transmitted flux for $F1$ phase function (n = 1.33, L = 2, ω = 0.95).

thick medium would differ little from that of optical thickness 10 in Fig. 11.

Finally, Fig. 13 reveals the effect of single-scattering albedo (ω) on the reflected intensity, for optical thicknesses equal to 10 and infinity. Figure 13 shows that the reflected intensity increases as the single-scattering albedo increases with the same optical thickness. This is a result of the same reason as discussed for Fig. 3. Moreover, the optical thickness effects are strong for ω = 1, and relatively insignificant for ω = 0.95. As can be seen, a small amount of absorption (ω = 0.95) causes little difference between the results for optical thicknesses of 10 and infinity, whereas no absorption (ω = 1.0) results in the need for a medium to have an optical thickness much greater than 10 to be termed optically thick.

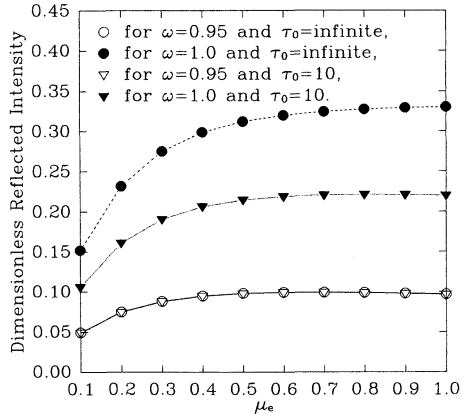

Fig. 13 Effect of single-scattering albedo on the nondimensional reflected intensity for $F1$ phase function (n = 1.33, L = 2).

Conclusions

Exact expressions for the source function, reflection and transmission functions, reflected and transmitted intensities, and fluxes at the boundaries of a plane–parallel medium are presented in this paper. This research was completed by using a procedure similar to that of Ambarzumian's method as well as employing superposition. The assumptions made were the following: no index of refraction effects at the lower boundary, no collimated incident radiation entering from the lower boundary, and incident azimuthal angle (ϕ_o) at the upper boundary being equal to zero.

For the semi-infinite case, the fundamental source function was expressed in terms of a set of simpler functions that could be solved by the successive approximation method. On the other hand, the fundamental source function of the finite case was expressed in terms of a set of dependent integro-differential equations. These equations include first-order derivatives, and can be solved by a combination of the Runge–Kutta numerical calculation method and the successive approximation method. Some selected numerical results are included to observe the effects of the albedo (0.95 and 1); refractive index (1 and 1.33); number of Legendre polynomials (0, 2, and 5); and optical thickness (up to 10, and infinity).

Future work will be directed toward adding the effects of polarization, because of the fact that polarization effects on the scattering medium can be significant.

References

[1]Haggag, M. H., Degheidy, A. R., and El-Depsy, A., "Efficient and Accurate Method for Radiation Transfer Problems," *Journal of Quantitative Spectroscopy and Radiative Transfer*, Vol. 58, No. 1, 1997, pp. 19–32.

[2]Liang, S., and Lewis, P., "A Parametric Radiative Transfer Model for Sky Radiance Distribution," *Journal of Quantitative Spectroscopy and Radiative Transfer*, Vol. 55, No. 2, 1996, pp. 181–189.

[3]Settle, J. J., "Some Exact Solutions for Coupled Atmosphere-Surface Radiation Models," *Journal of Quantitative Spectroscopy and Radiative Transfer*, Vol. 56, No. 1, 1996, pp. 47–55.

[4]Wang, Y., Mu, Y., and Ding, P., "A Linear Spline Approximation for Radiative Transfer Problems in Slab Medium," *Journal of Quantitative Spectroscopy and Radiative Transfer*, Vol. 55, No. 1, 1996, pp. 1–5.

[5]Wu, C., and Liou, B., "Radiative Transfer in a Two-Layer Slab with Fresnel Interfaces," *Journal of Quantitative Spectroscopy and Radiative Transfer*, Vol. 56, No. 4, 1996, pp. 573–589.

[6]Ambirajan, A., and Look, D. C., Jr., "A Backward Monte Carlo Estimator for the Multiple Scattering of a Narrow Light Beam," *Journal of Quantitative Spectroscopy and Radiative Transfer*, Vol. 56, No. 3, 1996, pp. 317–336.

[7]Reguigui, N. M., Dorri-Nowkoorani, F., Nobbmann, U., Ackerson, B. J., and Dougherty, R. L., "Correlation Transfer: Index of Refraction

and Anisotropy Effects," *Journal of Thermophysics and Heat Transfer*, Vol. 11, No. 3, 1997, pp. 400–408.

[8]Degheidy, A. R., "Radiative Transfer in a Scattering Medium with Angle-Dependent Reflective Boundaries," *Waves in Random Media*, Vol. 7, 1997, pp. 579–591.

[9]Crosbie, A. L., and Dougherty, R. L., "Two-Dimensional Isotropic Scattering in a Semi-Infinite Cylindrical Medium," *Journal of Quantitative Spectroscopy and Radiative Transfer*, Vol. 20, 1978, pp. 151–173.

[10]Crosbie, A. L., and Shieh, S. M., "Two-Dimensional Isotropic Scattering in a Semi-Infinite Cylindrical Medium with Refractive Index Greater than Unity," *Journal of Quantitative Spectroscopy and Radiative Transfer*, Vol. 49, No. 5, 1993, pp. 535–557.

[11]Crosbie, A. L., and Lee, L. C., "Two-Dimensional Anisotropic Scattering in a Semi-Infinite Cylindrical Medium Exposed to a Laser Beam," *Journal of Quantitative Spectroscopy and Radiative Transfer*, Vol. 49, No. 2, 1993, pp. 185–211.

[12]Crosbie, A. L., and Dougherty, R. L., "Two-Dimensional Radiative Transfer in a Cylindrical Geometry with Anisotropic Scattering," *Journal of Quantitative Spectroscopy and Radiative Transfer*, Vol. 25, 1980, pp. 551–569.

[13]Crosbie, A. L., and Dougherty, R. L., "Two-Dimensional Linearly Anisotropic Scattering in a Finite-Thick Cylindrical Medium Exposed to a Laser Beam," *Journal of Quantitative Spectroscopy and Radiative Transfer*, Vol. 33, No. 5, 1985, pp. 487–520.

[14]Crosbie, A. L., and Lee, L. C., "Single and Double Scattering Approximations for a Two-Dimensional Cylindrical Medium with Anisotropic Scattering," *Journal of Quantitative Spectroscopy and Radiative Transfer*, Vol. 48, No. 4, 1992, pp. 441–466.

[15]Reguigui, N. M., and Dougherty, R. L., "Two-Dimensional Radiative Transfer in a Cylindrical Layered Medium with Reflecting Boundaries," AIAA Paper 90-1779, June 1990.

[16]Ramankutty, M. A., and Crosbie, A. L., "Modified Discrete Ordinates Solution of Radiative Transfer in Two-Dimensional Rectangular Enclosures," *Journal of Quantitative Spectroscopy and Radiative Transfer*, Vol. 57, No. 1, 1997, pp. 107–140.

[17]Kim, T., and Lee, H., "Effect of Anisotropic Scattering on Radiative Heat Transfer in Two-Dimensional Rectangular Enclosures," *International Journal of Heat and Mass Transfer*, Vol. 31, No. 8, 1988, pp. 1711–1721.

[18]Kim, T., and Lee, H. S., "Radiative Transfer in Two-Dimensional Anisotropic Scattering Media with Collimated Incidence," *Journal of Quantitative Spectroscopy and Radiative Transfer*, Vol. 42, No. 3, 1989, pp. 225–238.

[19]Mitra, K., Lai, M., and Kumar, S., "Transient Radiation Transport in Participating Media Within a Rectangular Enclosure," *Journal of Thermophysics and Heat Transfer*, Vol. 11, No. 3, 1997, pp. 409–414.

[20]Crosbie, A. L., and Shieh, S. M., "Three-Dimensional Radiative Transfer for Anisotropic Scattering Medium with Refractive Index Greater than Unity," *Journal of Quantitative Spectroscopy and Radiative Transfer*, Vol. 44, No. 2, 1990, pp. 299–312.

[21]Kim, M. Y., and Baek, S. W., "Analysis of Radiative Transfer in Cylindrical Enclosures Using the Finite Volume Method," *Journal of Thermophysics and Heat Transfer*, Vol. 11, No. 2, 1997, pp. 246–252.

[22]Spuckler, C. M., and Siegel, R., "Refractive Index Effects on Radiative Behavior of a Heated Absorbing-Emitting Layer," *Journal of Thermophysics and Heat Transfer*, Vol. 6, No. 4, 1992, pp. 596–604.

[23]Spuckler, C. M., and Siegel, R., "Refractive Index and Scattering Effects on Radiation in a Semitransparent Laminated Layer," *Journal of Thermophysics and Heat Transfer*, Vol. 8, No. 2, 1994, pp. 193–201.

[24]Siegel, R., and Spuckler, C. M., "Variable Refractive Index Effects on Radiation in Semitransparent Scattering Multilayered Regions," *Journal of Thermophysics and Heat Transfer*, Vol. 7, No. 4, 1993, pp. 624–630.

[25]Siegel, R., "Refractive Index Effects on Transient Cooling of a Semitransparent Radiating Layer," *Journal of Thermophysics and Heat Transfer*, Vol. 9, No. 1, 1995, pp. 55–62.

[26]Siegel, R., "Transient Emittance Limit for Cooling a Semitransparent Radiating Layer," *Journal of Thermophysics and Heat Transfer*, Vol. 9, No. 2, 1994, pp. 373–375.

[27]Siegel, R., "Refractive Index Effects on Local Radiative Emission from a Rectangular Semitransparent Solid," *Journal of Thermophysics and Heat Transfer*, Vol. 8, No. 3, 1993, pp. 625–628.

[28]Dougherty, R. L., "Radiative Transfer in a Semi-Infinite Absorbing/Scattering Medium with Reflective Boundary," *Journal of Quantitative Spectroscopy and Radiative Transfer*, Vol. 41, No. 1, 1989, pp. 55–67.

[29]Liu, C,-C., "Numerical Calculation of Radiative Transfer in One-Dimensional Media with a Reflective Top Boundary and Anisotropic Scattering," M.S. Thesis, Oklahoma State Univ., Stillwater, OK, 1993.

[30]Ambarzumian, V. A., "Diffusion of Light by Planetary Atmospheres," *Astronomical Journal of the Soviet Union*, Vol. 19, 1942, pp. 30–41.

[31]Dorri-Nowkoorani, F., Tian, Y., Reguigui, N. M., Nobbmann, U., Ackerson, B. J., and Dougherty, R. L., "Improved P_n Approximation for One-Dimensional Scattering and Absorbing Media with Application to Correlation Transfer," AIAA Paper 94-2096, June 1994.